usual memory demand associated with matrix inversion techniques.

J.-M. JIN
J. L. VOLAKIS

Radiation Laboratory
Department of Electrical Engineering & Computer Science
University of Michigan
Ann Arbor, MI 48109, USA

20th June 1989

References

1 AUCKLAND, D. T., and HARRINGTON, R. F.: 'A nonmodal formulation for electromagnetic transmission through a filled slot of arbitrary cross section in a thick conducting screen', *IEEE Trans. Microw. Theory Tech.*, 1980, **28**, pp. 548–555

2 AUCKLAND, D. T., and HARRINGTON, R. F.: 'Electromagnetic transmission through a filled slit in a conducting plane of finite thickness, TE case', *IEEE Trans. Micro. Theory Tech.*, 1978, **26**, pp. 499–505

3 WANG, N.: 'Electromagnetic scattering from a filled slit in a thick conducting screen, TM case'. The Ohio State Univ. ElectroScience Lab. Tech. Report 714349-8, May 1984

LOW-THRESHOLD ELECTRICALLY PUMPED VERTICAL-CAVITY SURFACE-EMITTING MICROLASERS

Indexing terms: Semiconductor lasers, Quantum optics

Vertical-cavity electrically driven lasers with three GaInAs quantum wells and diameters of several μm exhibit room-temperature pulsed current thresholds as low as 1·3 mA with 958 nm output wavelength.

Vertical-cavity surface-emitting lasers[1–3] show promise for a variety of applications. The lowest threshold edge-emitting lasers contain a single quantum well and require approximately 0·55 mA for operation.[4–6] Optically pumped vertical-cavity lasers with μm dimenions[7] have shown promise for much lower thresholds, especially if only a few, or even one, quantum well is used.[8]

We have constructed a large number of electrically pumped vertical-cavity surface-emitting semiconductor lasers with dimensions of a few μm (μ-lasers) on a single GaAs chip. Diameters are 2, 3, 4 and 5 μm and heights are 5·5 μm. The yield is between 95 and 100% for 5 μm diameter devices in all examined regions. Pulsed thresholds range from 1·3 mA (3 μm diameter) to 2 mA (5 μm diameter). The device density is about two million per cm^2. The chip size is about 3 × 5 mm.

Molecular beam epitaxy was used to grow the sample. The substrate was Si-doped n^+-GaAs on which alternate layers of AlAs and GaAs were grown, forming an interference mirror. These layers, each nominally a 1/4-wave optical thickness at 980 nm, were Si-doped at 3×10^{18} cm^{-3}. The undoped active region consists of three 80 Å $Ga_{0.8}In_{0.2}As$ quantum wells interleaved with four 100 Å GaAs barriers. Surrounding the active region are 200 Å compositionally graded[9] undoped $Al_xGa_{1-x}As$ layers with x ranging from 0 to 0·5. Above and below the graded layer active region complex are spacer regions of doped $Al_{0.5}Ga_{0.5}As$ of thicknesses so that a full wave exists between mirrors. The second mirror was constructed similarly to the first using Be as the dopant. The innermost three layers of the second mirror, where the optical intensity is highest, were doped at 2.5×10^{18} cm^{-3}, whereas the remaining outermost layers were doped at 5×10^{18} cm^{-3}. The Si-doped mirror had 20 half-wave periods; the Be-doped mirror had 12. Above the Be-doped mirror were grown a ~0·2 optical wave thickness of AlAs and a 30 Å GaAs cap of GaAs, both Be-doped at 5×10^{18} cm^{-3}. For low contact resistance, the cap was also delta-doped[10] with 10^{13} cm^{-3} of Be. The cap layer was covered with unalloyed Au, 1500 Å thick.

Standard contact photolithography with liftoff was used to create circular spots of Ni, 1–5 μm diameter, on the Au. Chemical beam ion-beam-assisted etching was used to etch through the Au and the 5·35 μm heterostructure, leaving the Ni covered areas. The Ni thickness was chosen so that it barely eroded away.

The other side of substrate was polished and a wire serving as ground was spot-welded to it. Positive voltage pulses were applied to the Au caps using a small probe tip of radius ~5 μm. Laser outputs went through the substrate and out the polished side. Luminescence was unpolarised and the laser light was linearly polarised.

Fig. 1 displays output light at 958 nm against driving current for a 3 μm μ-laser. Voltage pulses were 50 ns at low

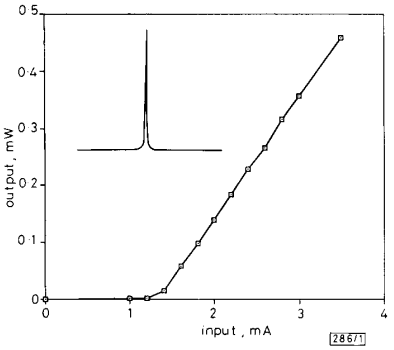

Fig. 1 *Output light power against current*

Differential quantum efficiency is about 16%. Inset shows typical spectrum at 1·6 mA for a 3 μm diameter microlaser. Peak full width at half-maximum is about 4 Å, the spectrometer resolution. Trace spans from 9300 to 9845 Å

duty cycle. The measured single-facet differential quantum efficiency was about 16%, despite some absorption of the laser output in the doped substrate. At threshold the voltage was about 15 V, rising to 20 V at 3·5 mA. The 5 μm μ-lasers required about 8 V and 2 mA for threshold. This very low 1·3 mA current threshold was obtained despite very fast expected carrier recombination due to surface recombination.[11] The fast carrier recombination and high mirror resistances caused substantial heating preventing room-temperature CW operation. No heat-sinking was used. We did operate with duty cycle as high as 40%. The reduction of current thresholds would reduce both the voltage drop and device heating. The inset shows a spectrum taken using 50 ns 1·6 mA pulses. During a single longer pulse operation, wavelength shifts of 25 Å were observed, corresponding to a 50°C temperature rise. Lasing wavelength variations of ±15 Å were noted upon driving lasers on different portions of the chip.

Fig. 2 displays the output pulse train obtained when a

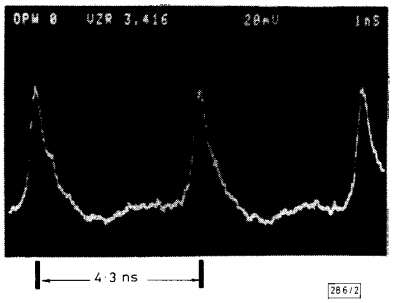

Fig. 2 *Laser output light pulses when driven by continuous 230 MHz voltage sine wave*

Detection system used Si avalanche photodiode and sampling oscilloscope. Observed 100 ps rise time is approximately response time of system

μ-laser was driven with a continuous 230 MHz voltage sine wave.

Surface recombination should be much less important with GaInAsP compounds used for lasers with 1·55 μm wavelength output. The suppression of surface recombination[12] should allow current thresholds less than 10 μA in smaller devices. Reduced threshold current, improved heat-sinking, or lower resistance mirrors should also allow room temperature CW operation.

We thank R. Martin for the spot-welding to the substrate.

J. L. JEWELL
A. SCHERER*
S. L. McCALL†
Y. H. LEE
S. WALKER
J. P. HARBISON*
L. T. FLOREZ*

AT&T Bell Laboratories
Holmdel, NJ 07733, USA

* *Bellcore*
Red Bank, NJ 07701, USA

† *AT&T Bell Laboratories*
Murray Hill, NJ 07974, USA

19th June 1989

References

1 KINOSHITA, S., MORITO, K., KOYAMA, F., and IGA, K.: 'Reproducible fabrication of AlAs/GaAs circular buried heterostructure (CBH) surface-emitting lasers with low threshold', *Electron. Lett.*, 1988, **24**, pp. 699–700

2 SAKAGUCHI, T., KOYAMA, F., and IGA, K.: 'Vertical cavity surface-emitting laser with AlGaAs/AlAs Bragg reflector', *Electron. Lett.*, 1988, **24**, pp. 928–929

3 KOYAMA, F., KINOSHITA, S., and IGA, K.: 'Room temperature cw vertical cavity surface emitting laser and high power 2-D laser array', *Tech. Dig., CLEO '89* (Optical Society of America, Baltimore), paper FC1

4 DERRY, P. L., YARIV, A., LAU, K. Y., BAR-CHAIM, N., LEE, K., and ROSENBERG, J.: 'Ultralow-threshold graded-index separate-confinement single quantum well buried heterostructure (Al, Ga)As lasers with high reflectivity coatings', *Appl. Phys. Lett.*, 1987, **50**, pp. 1773–1775

5 LAU, K. Y., DERRY, P. L., and YARIV, A.: 'Ultimate limit in low threshold quantum well GaAlAs semiconductor lasers', *Appl. Phys. Lett.*, 1988, **52**, pp. 88–90

6 YARIV, A.: 'Scaling laws and minimum threshold currents for quantum-confined semiconductor lasers', *Appl. Phys. Lett.*, 1988, **53**, pp. 1033–1035

7 JEWELL, J. L., MCCALL, S. L., LEE, Y. H., SCHERER, A., GOSSARD, A. C., and ENGLISH, J. H.: 'Lasing characteristics of GaAs microresonators', *Appl. Phys. Lett.*, 1988, **54**, pp. 1400–1402

8 JEWELL, J. L., HUANG, K. F., TAI, K., LEE, Y. H., FISHER, R. J., MCCALL, S. L., and CHAO, A. Y.: 'Vertical cavity single quantum well laser', *Appl. Phys. Lett.*, 1989

9 TSANG, W. T.: 'Extremely low threshold AlGaAs graded index waveguide separate confinement heterostructure lasers grown by molecular beam epitaxy', *Appl. Phys. Lett.*, 1982, **40**, pp. 217–219

10 SCHUBERT, E. F., CUNNINGHAM, J. E., and CHIU, T. H.: 'Delta-doped ohmic contacts to n-GaAs', *Appl. Phys. Lett.*, 1986, **49**, pp. 292–294

11 JEWELL, J. L., SCHERER, A., MCCALL, S. L., GOSSARD, A. C., and ENGLISH, J. H.: 'GaAs-AlAs monolithic microresonator arrays', *Appl. Phys. Lett.*, 1987, **51**, pp. 94–96

12 SANDROFF, C. J., HEDGE, M. S., FARROW, L. A., CHANG, C. C., and HARBISON, J. P.: 'Electronic passivation of GaAs surfaces through the formation of arsenic—sulfur bonds', *Appl. Phys. Lett.*, 1989, **54**, pp. 362–364

HIGH-FREQUENCY PERFORMANCE OF MOVPE *npn* AlGaAs/GaAs HETEROJUNCTION BIPOLAR TRANSISTORS

Indexing terms: Semiconductor devices and materials, Bipolar devices, Transistors, Epitaxy

Base doping densities near $10^{20}\,cm^{-3}$ and emitter doping densities near $7 \times 10^{17}\,cm^{-3}$ have been achieved in MOVPE HBT structures and combined with self-aligned processing resulting in $f_{max} = 94$ GHz and $f_t = 45$ GHz. To our knowledge, these are the first MOVPE HBTs demonstrated to operate at millimetre-wave frequencies.

Introduction: The heterojunction bipolar transistor is a promising high-speed device.[1-2] The realisation of this high-speed performance is dependent on the reduction of parasitic delays. These delays can be reduced with a combination of self-aligned processing which reduces extrinsic parasitics and high doping densities in the emitter, base and collector which reduce the contact, spreading and intrinsic resistances.

Epitaxial growth: The HBT structure was grown by MOVPE at 40 Torr and 550°C. It consisted of a superlattice buffer, 6000 Å $1 \times 10^{19}\,cm^{-3}$ Te-doped GaAs subcollector, 5000 Å $5 \times 10^{16}\,cm^{-3}$ Si-doped GaAs collector, 800 Å $1 \times 10^{20}\,cm^{-3}$ Zn-doped GaAs base, 200 Å undoped GaAs spacer, 2000 Å $7 \times 10^{17}\,cm^{-3}$ Te-doped $Al_{0.30}Ga_{0.70}As$ emitter including 300 Å of emitter-base grading and 500 Å of emitter-contact grading and a 1000 Å $1 \times 10^{19}\,cm^{-3}$ Te-doped GaAs emitter contact layer. A detailed study on the growth of HBT structures with these high doping densities will be presented elsewhere.[3]

Device fabrication: A fully self-aligned dual liftoff process,[4] which had generated the best performing MBE HBTs, was employed to fabricate MOVPE HBTs. Inasmuch as the same process was employed to fabricate both MOVPE and MBE HBTs, a direct comparison can be made between HBTs grown by these two different epitaxial technologies. The dual liftoff process is capable of generating small geometry HBTs (emitter width down to 1·2 μm) with low device parasitics while maintaining a high throughput optical lithography. Critical processing steps of the dual liftoff process can be summarised as follows.

After device isolation, a single photoresist pattern was used to define an etch-down to the base layer of a HBT structure, thereby establishing the active emitter area. The same photoresist was used in masking the photon implantation for base-collector capacitance reduction and the base metal evaporation. Finally, the photoresist was used to mask a low-temperature-deposited dielectric (Photo-CVD Si_3N_4). The base metal and the dielectric were patterned by liftoff as the photoresist is dissolved. The resultant structure had base metal in base contact areas overlaid with a dielectric which protected both the metal and the sidewalls. This process was termed 'dual liftoff' because unwanted base metal and dielectric were lifted off concurrently. Following the liftoff, one can use noncritical alignment to define an emitter contact pattern because the emitter metal can overlap the covered extrinsic base area or the base contact area without concern for emitter-base shorting. Contact to the collector was made by etching a via hole through the uppermost layers down to the buried subcollector. Polyimide was used to form the interlayer dielectric and two levels of interconnect metal were provided. All lithographic work was carried out with an optical contact aligner.

Device performance: The self-aligned dual lift off process has generated MOVPE HBTs with minimum device parasitics and excellent RF performances. According to the transmission line measurement on fabricated MOVPE HBT wafers, the sheet resistance of the base layer was found to be 124 Ω/sq, corresponding to a base layer doping density of $1 \times 10^{20}/cm^3$ (as quantified by the Hall measurement). The base contact resistance was extrapolated to be $5{\cdot}1 \times 10^{-7}\,\Omega\,cm^2$. Making use of Te as *n*-type dopant, we were able to reduce both emitter and subcollector resistances by increasing doping densities up to $1 \times 10^{19}/cm^3$. The contact resistances of the emitters and subcollectors were measured to be $4{\cdot}7 \times 10^{-7}\,\Omega\,cm^2$ and $5{\cdot}3 \times 10^{-7}\,\Omega\,cm^2$, respectively. The measured sheet resist-